

Supporting information

Paradigm for efficient synthesis of bio-based polycarbonate with deep eutectic solvents as catalysts by inhibiting the degradation of molecular chains

Weiwei Wang ^{a,b}, Zifeng Yang ^{a,b}, Yaqin Zhang ^a, Hongyan He ^{a,b,c}, Wenjuan Fang ^a, Zhencai Zhang ^b and Fei Xu ^{*a,b,c,d}

^a CAS Key Laboratory of Green Process and Engineering, State Key Laboratory of Multiphase Complex Systems, Beijing Key Laboratory of Ionic Liquids Clean Process, Institute of Process Engineering, Chinese Academy of Sciences, Beijing 100190, China.

^b School of Chemical Engineering, University of Chinese Academy of Sciences, Beijing 100049, China.

^c Dalian National Laboratory for Clean Energy, Dalian 116023, China.

^d Zhongke Langfang Institute of Process Engineering, Langfang 065001, China.

E-mail: fxu@ipe.ac.cn;

Characterization of DESs

[EminOH]Cl

^1H NMR (600 MHz, DMSO) δ 9.19 (s, 1H), 7.79 (d, $J = 1.7$ Hz, 1H), 7.75 (d, $J = 1.7$ Hz, 1H), 5.49 (s, 1H), 4.26 – 4.22 (m, 2H), 3.87 (s, 3H), 3.70 (d, $J = 5.0$ Hz, 2H). FT-IR (KBr) ν : 3439, 3145, 3057, 2955, 2871, 1649, 1568, 1444, 1347, 1169, 1067, 937, 1067, 862, 787, 746, 613 cm^{-1} .

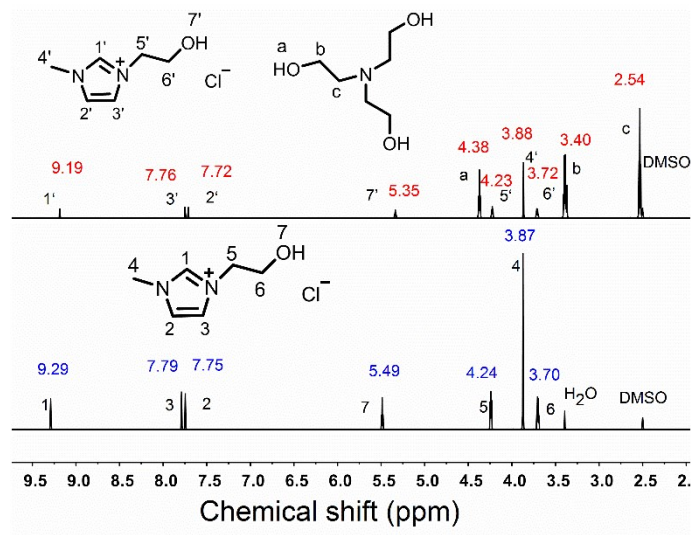


Figure S1. ^1H NMR spectra of [EminOH]Cl-2TEOA and [EminOH]Cl.

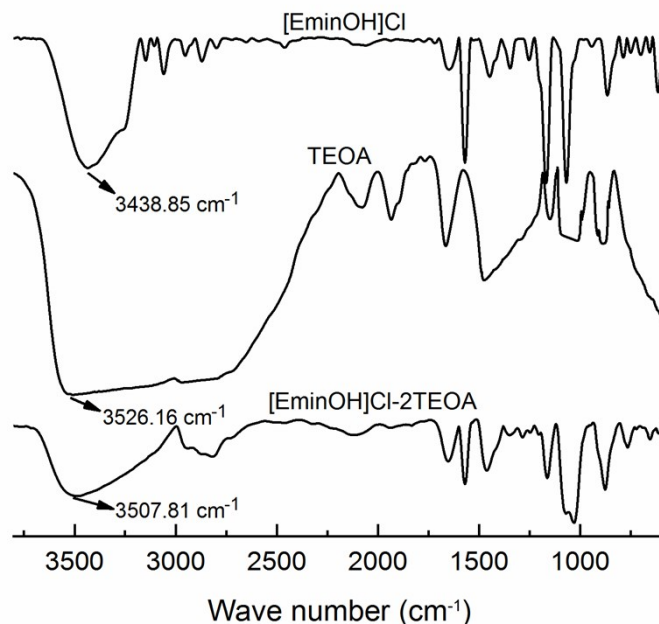


Figure S2. FT-IR spectra of [EminOH]Cl, TEOA and [EminOH]Cl-2TEOA.

[EminOH]Cl-2TEOA

^1H NMR (600 MHz, DMSO) δ 9.19 (s, 1H), 7.76 (t, $J = 1.7$ Hz, 1H), 7.72 (t, $J = 1.7$ Hz, 1H), 5.35 (s, 1H), 4.38 (t, $J = 5.6$ Hz, 6H), 4.25 – 4.21 (m, 2H), 3.88 (s, 3H), 3.72 (d, $J = 5.0$ Hz, 2H), 3.40 (q, $J = 6.0$ Hz, 12H), 2.54 (t, $J = 6.2$ Hz, 12H). FT-IR

(KBr) ν : 3508, 2949, 3057, 2817, 2114, 1655, 1573, 1459, 1354, 1287, 1164, 1031, 870, 770, 650 cm^{-1} .

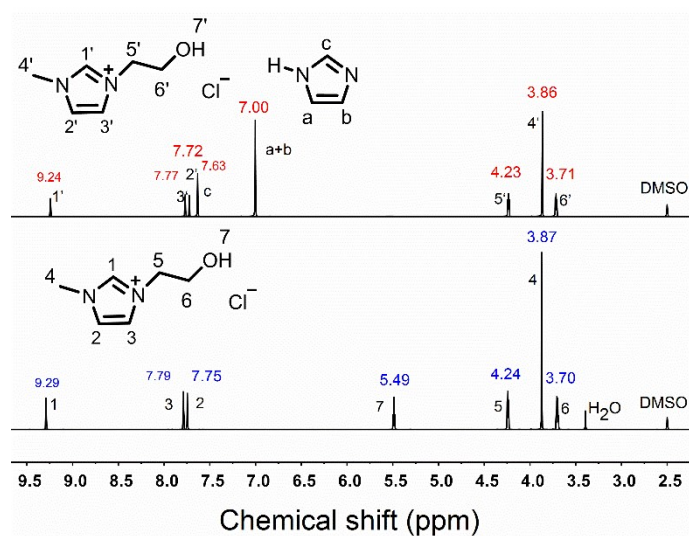


Figure S3. ^1H NMR spectra of $[\text{EminOH}]\text{Cl}\cdot 2\text{IM}$ and $[\text{EminOH}]\text{Cl}$.

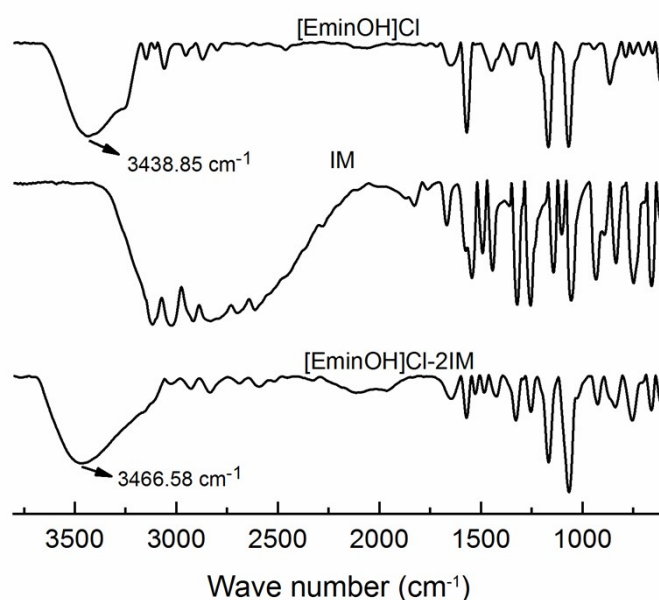


Figure S4. FT-IR spectra of $[\text{EminOH}]\text{Cl}$, IM and $[\text{EminOH}]\text{Cl}\cdot 2\text{IM}$.

$[\text{EminOH}]\text{Cl}\cdot 2\text{IM}$

^1H NMR (600 MHz, DMSO) δ 9.24 (s, 1H), 7.77 (t, $J = 1.7$ Hz, 1H), 7.72 (t, $J = 1.7$ Hz, 1H), 7.63 (s, 2H), 7.00 (d, $J = 0.8$ Hz, 4H), 4.23 (dd, $J = 6.6, 3.5$ Hz, 2H), 3.86 (s, 3H), 3.75 – 3.67 (m, 2H). FT-IR (KBr) ν : 3467, 3021, 2932, 2833, 1647, 1572, 1522, 1481, 1429, 1325, 1254, 1164, 1062, 927, 846, 757, 663, 613 cm^{-1} .

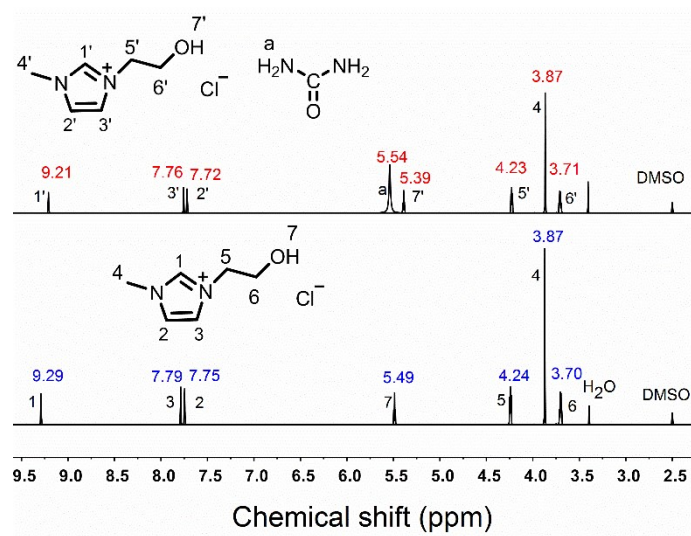


Figure S5. ^1H NMR spectra of $[\text{EminOH}]\text{Cl}\cdot 2\text{UREA}$ and $[\text{EminOH}]\text{Cl}$.

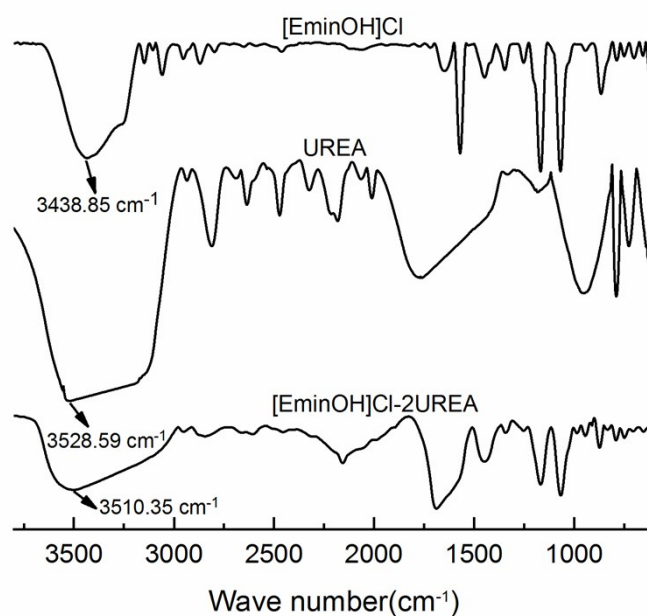


Figure S6. FT-IR spectra of $[\text{EminOH}]\text{Cl}$, UREA and $[\text{EminOH}]\text{Cl}\cdot 2\text{UREA}$.

$[\text{EminOH}]\text{Cl}\cdot 2\text{UREA}$

^1H NMR (600 MHz, DMSO) δ 9.21 (s, 1H), 7.76 (t, $J = 1.7$ Hz, 1H), 7.72 (t, $J = 1.7$ Hz, 1H), 5.54 (s, 8H), 5.39 (t, $J = 5.3$ Hz, 1H), 4.25 – 4.18 (m, 2H), 3.87 (s, 3H), 3.71 (dd, $J = 10.2, 5.2$ Hz, 2H). FT-IR (KBr) ν : 3510, 2957, 2849, 2154, 1686, 1449, 1339, 1250, 1163, 1070, 871, 786, 745 cm^{-1} .

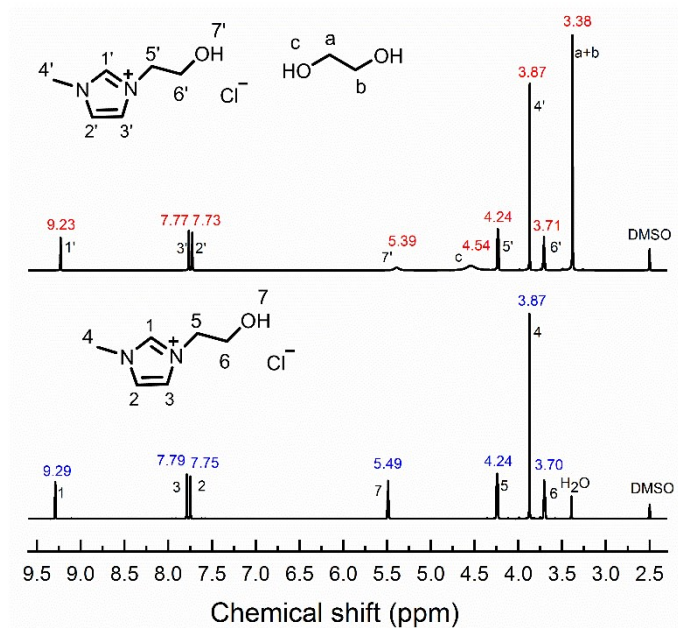


Figure S7. ^1H NMR spectra of $[\text{EminOH}]\text{Cl}\cdot 2\text{EG}$ and $[\text{EminOH}]\text{Cl}$.

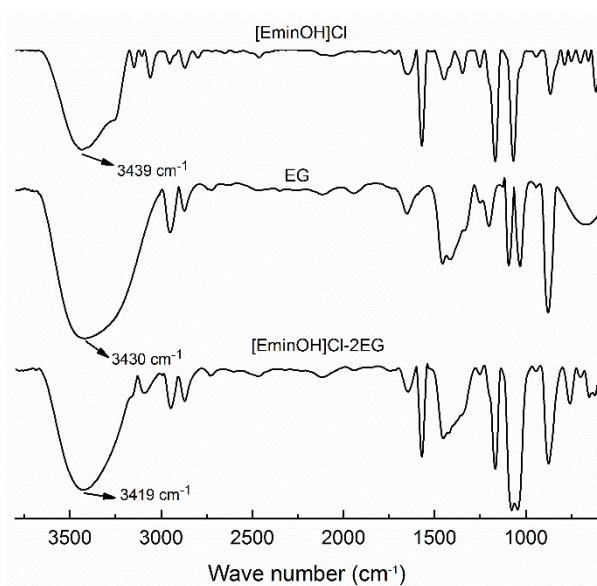


Figure S8. FT-IR spectra of $[\text{EminOH}]\text{Cl}$, EG and $[\text{EminOH}]\text{Cl}\cdot 2\text{EG}$.

$[\text{EminOH}]\text{Cl}\cdot 2\text{EG}$

^1H NMR (600 MHz, DMSO) δ 9.23 (s, 1H), 7.77 (t, $J = 1.7$ Hz, 1H), 7.73 (t, $J = 1.7$ Hz, 1H), 5.39 (s, 1H), 4.54 (s, 4H), 4.23 (dd, $J = 6.6, 3.5$ Hz, 2H), 3.87 (s, 3H), 3.74 – 3.68 (m, 2H), 3.38 (s, 8H). FT-IR (KBr) ν : 3419, 3093, 2941, 2876, 1645, 1574, 1449, 1165, 1063, 871, 756, 653 cm^{-1} .

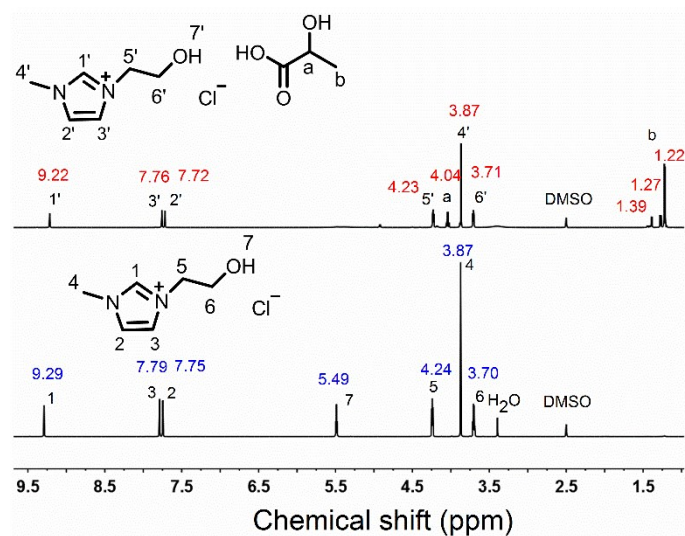


Figure S9. ^1H NMR spectra of [EminOH]Cl-2LA and [EminOH]Cl.

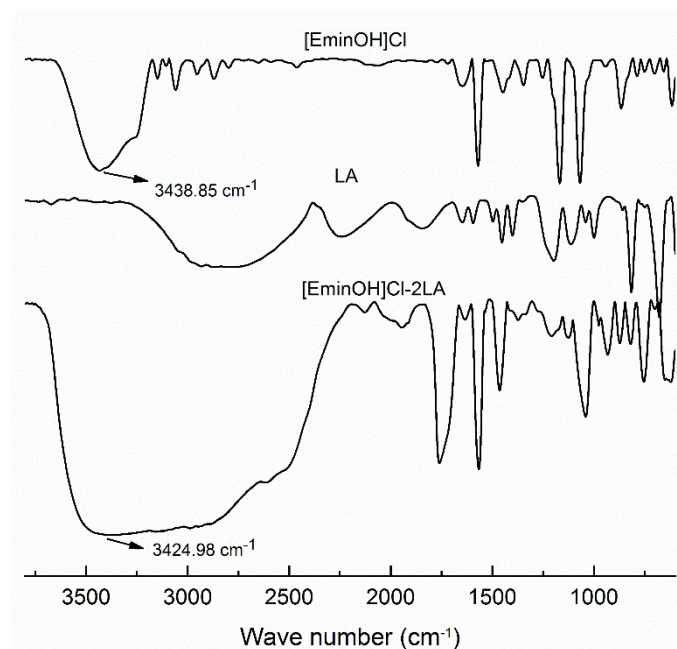


Figure S10. FT-IR spectra of [EminOH]Cl, LA and [EminOH]Cl-2LA.

[EminOH]Cl-2LA

^1H NMR (600 MHz, DMSO) δ 9.22 (s, 1H), 7.76 (t, $J = 1.7$ Hz, 1H), 7.72 (t, $J = 1.7$ Hz, 1H), 4.23 (dd, $J = 6.6, 3.5$ Hz, 2H), 4.04 (q, $J = 6.9$ Hz, 2H), 3.87 (d, $J = 8.3$ Hz, 3H), 3.72 – 3.69 (m, 2H), 1.39 (d, $J = 7.1$ Hz, 1H), 1.27 (d, $J = 6.9$ Hz, 1H), 1.22 (d, $J = 6.9$ Hz, 4H). FT-IR (KBr) ν : 3425 2134 1946 1759 1566 1462 1373 1204 1129 1045 932 871 815 754 631 cm^{-1} .

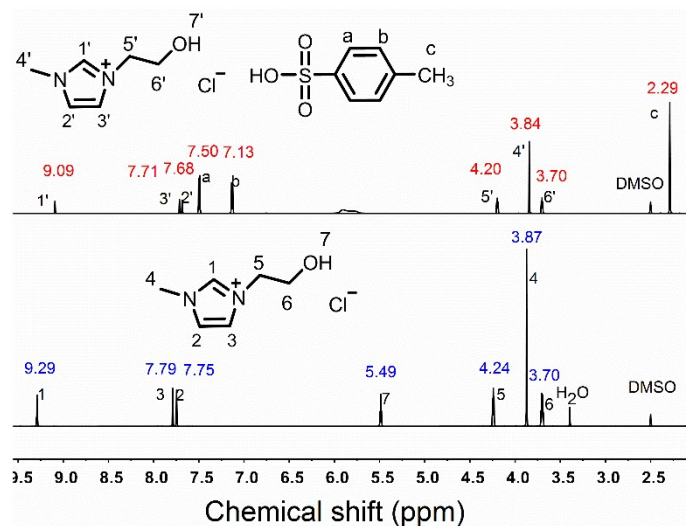


Figure S11. ^1H NMR spectra of $[\text{EminOH}]\text{Cl}\cdot 2\text{PTSA}$ and $[\text{EminOH}]\text{Cl}$.

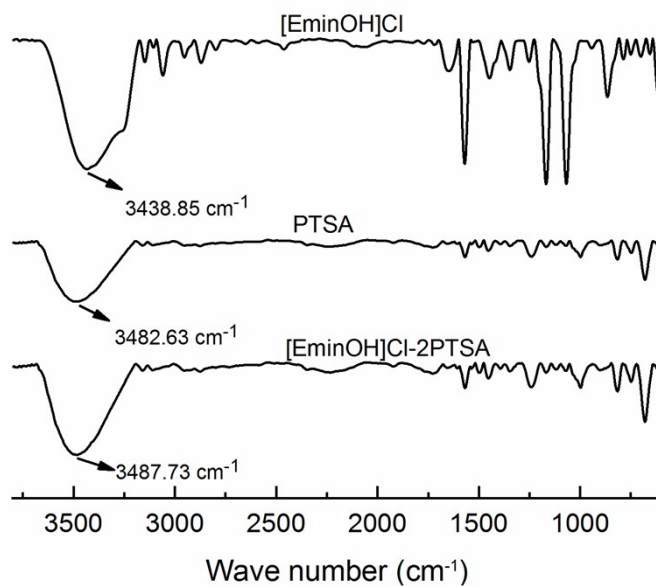


Figure S12. FT-IR spectra of $[\text{EminOH}]\text{Cl}$, PTSA and $[\text{EminOH}]\text{Cl}\cdot 2\text{PTSA}$.

$[\text{EminOH}]\text{Cl}\cdot 2\text{PTSA}$

^1H NMR (600 MHz, DMSO) δ 9.09 (s, 1H), 7.71 (t, $J = 1.6$ Hz, 1H), 7.68 (t, $J = 1.5$ Hz, 1H), 7.50 (d, $J = 8.1$ Hz, 4H), 7.13 (d, $J = 7.9$ Hz, 4H), 4.22 – 4.18 (m, 2H), 3.84 (s, 3H), 3.71 – 3.69 (m, 2H), 2.29 (s, 6H). FT-IR (KBr) ν : 3419 3093 2941 2876 1645 1574 1449 1165 1063 871 756 653 cm^{-1} .

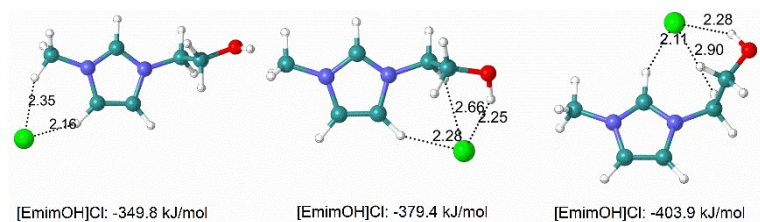


Figure S13. Possible hydrogen bonding network structure between the anion and the cation of [EminOH]Cl.

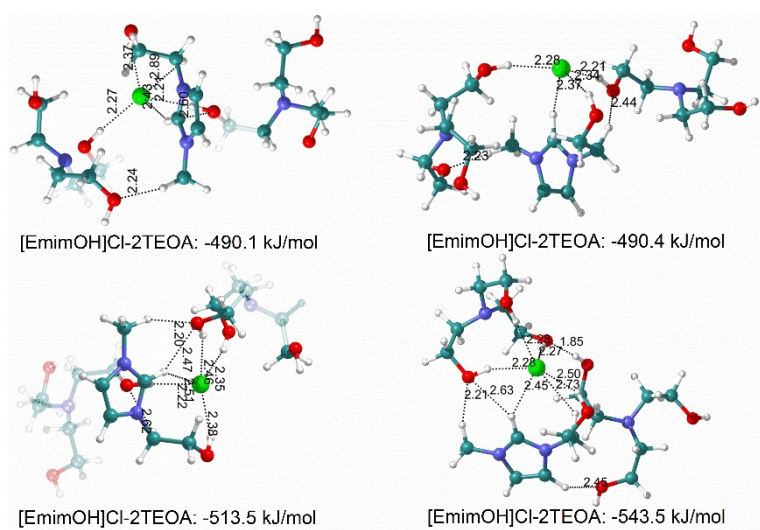


Figure S14. Possible hydrogen bonding network structure between [EminOH]Cl and TEOA.

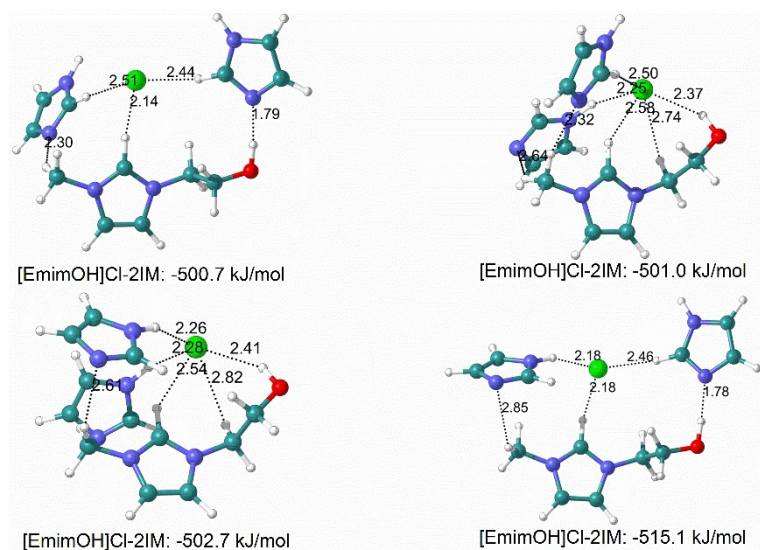


Figure S15. Possible hydrogen bonding network structure between [EminOH]Cl and IM.

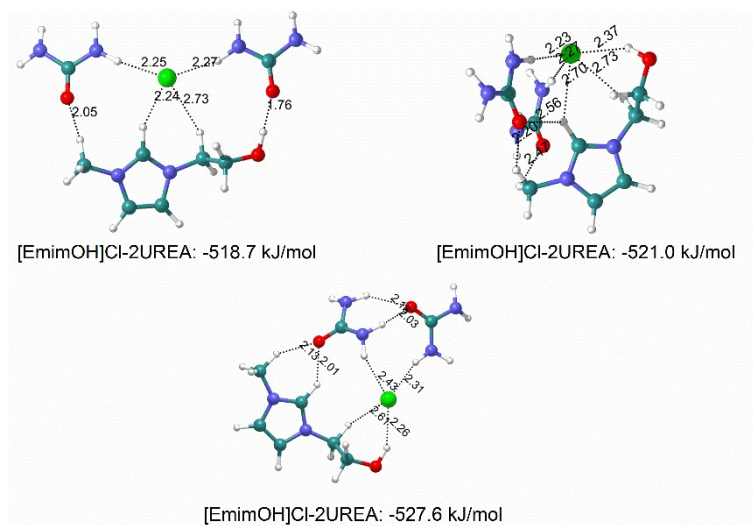


Figure S16. Possible hydrogen bonding network structure between [EmimOH]Cl and UREA.

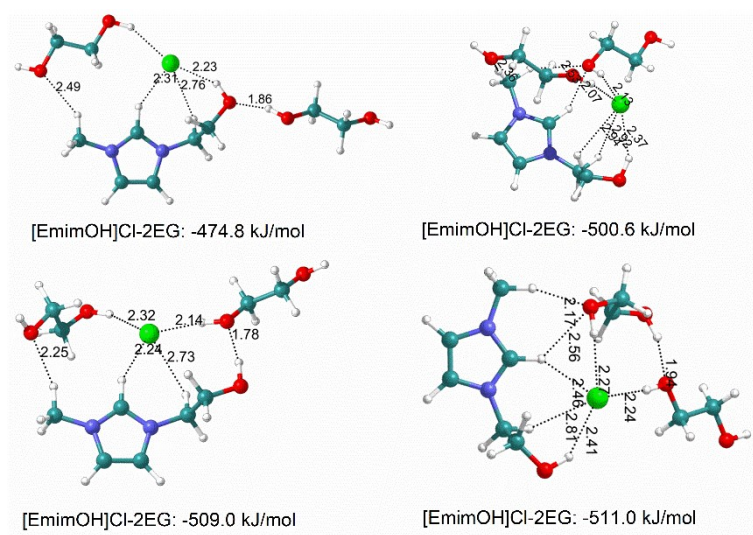


Figure S17. Possible hydrogen bonding network structure between [EmimOH]Cl and EG.

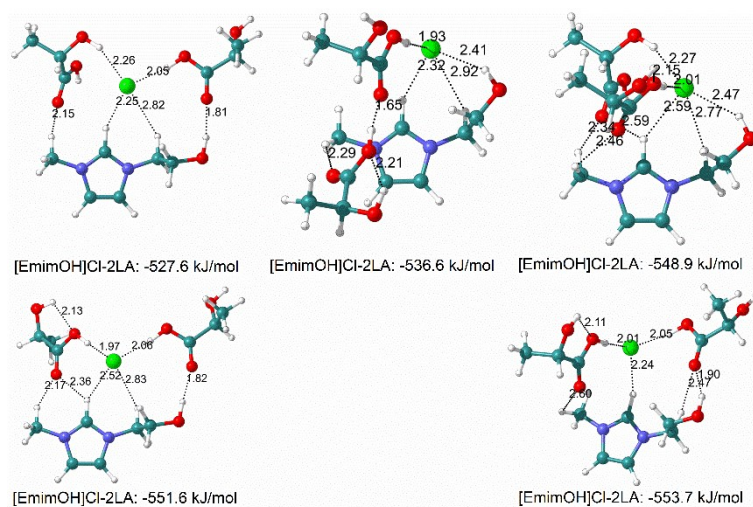


Figure S18. Possible hydrogen bonding network structure between [EmimOH]Cl and LA.

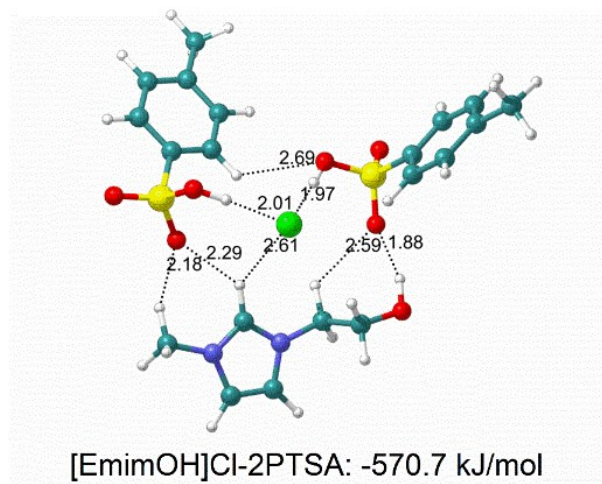


Figure S19. Possible hydrogen bonding network structure between [EminOH]Cl and PTSA.

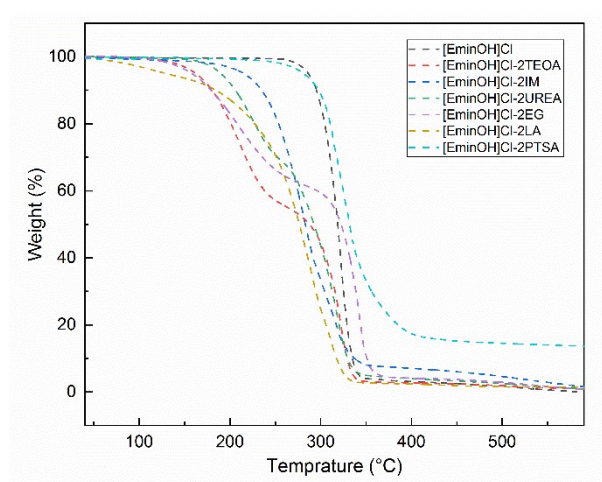


Figure S20. TGA curve of the catalysts.

Table S1 Thermal decomposition temperature of the catalysts

Entry	Catalyst	T _{50%} ^a (°C)
1	[EminOH]Cl	319
2	[EminOH]Cl-2TEOA	323
3	[EminOH]Cl-2IM	292
4	[EminOH]Cl-2UREA	283
5	[EminOH]Cl-2EG	288
6	[EminOH]Cl-2LA	282
7	[EminOH]Cl-2PTSA	332

^a The temperature when the weight loss reached 50%.

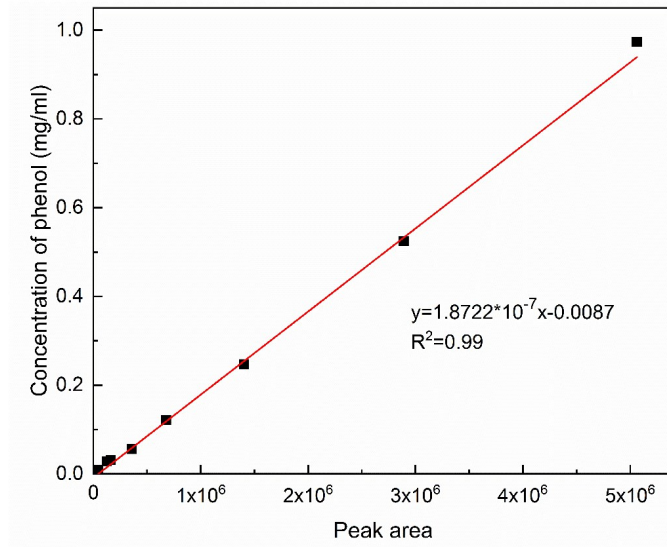


Figure S21. Standard curve equation between peak area and phenol concentration.

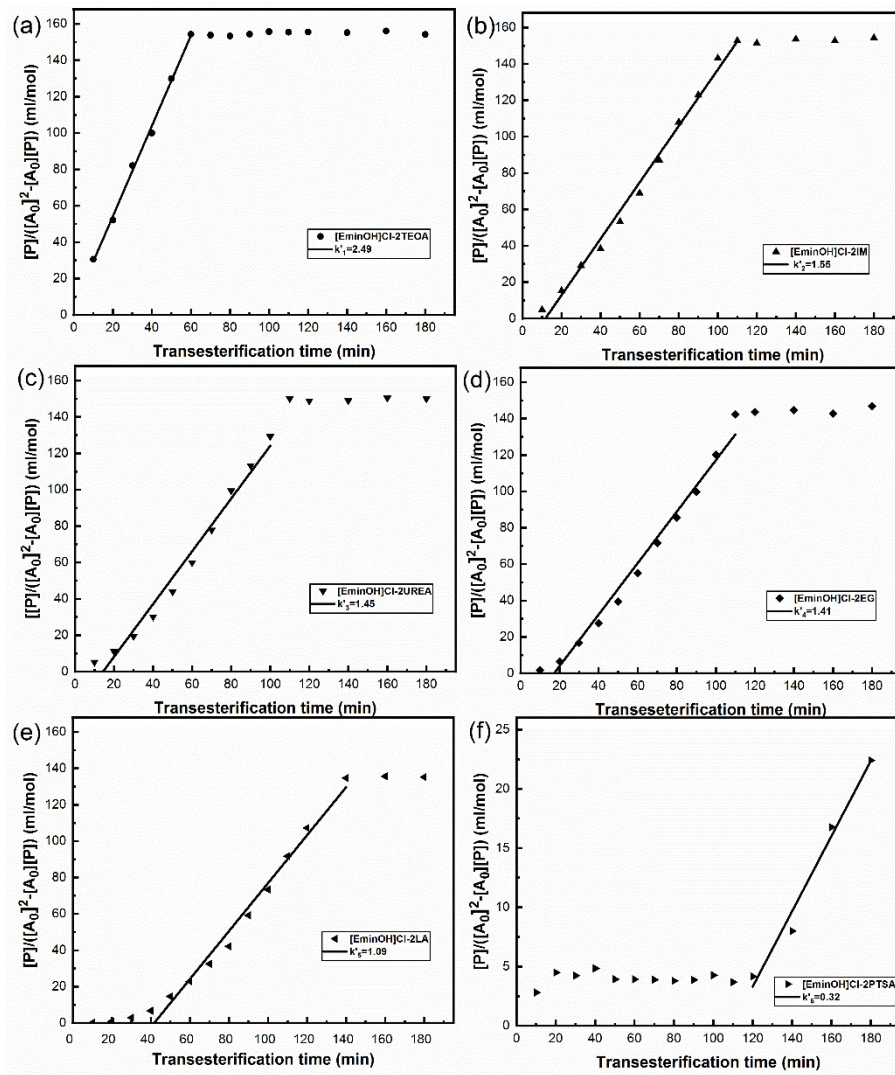


Figure S22. k' (slope) catalyzed by different DESs at 140 °C.

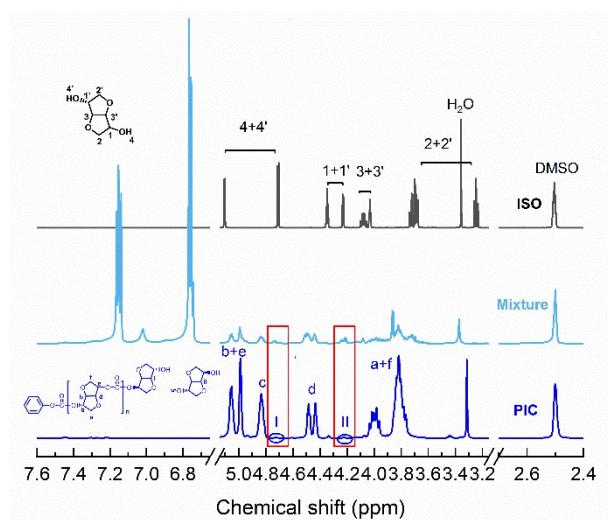


Figure S23. ^1H NMR spectra of ISO, pure PIC and degradation mixture with $[\text{EminOH}]\text{Cl-2IM}$.

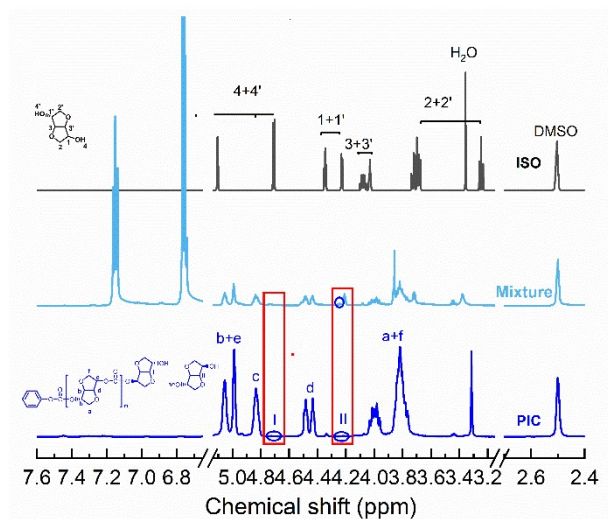


Figure S24. ^1H NMR spectra of ISO, pure PIC and degradation mixture with $[\text{EminOH}]\text{Cl-2UREA}$.

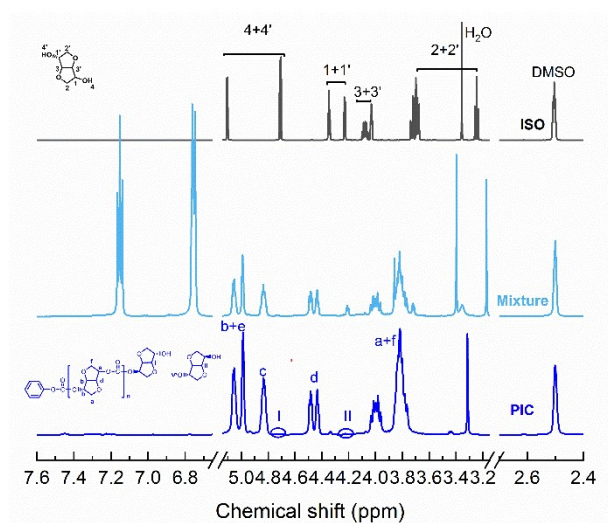


Figure S25. ^1H NMR spectra of ISO, pure PIC and degradation mixture with $[\text{EminOH}]\text{Cl-2EG}$.

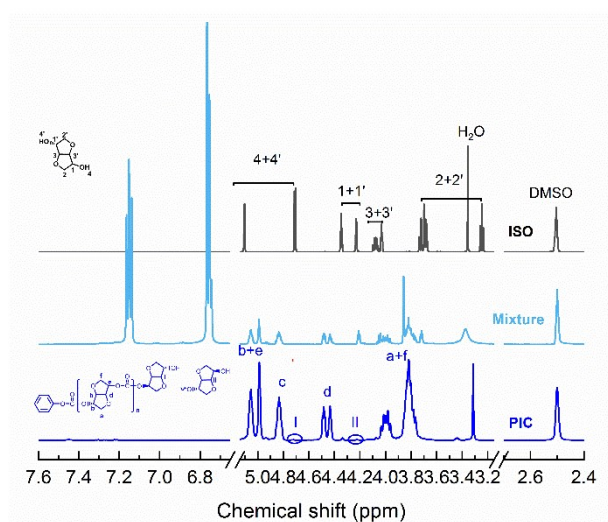


Figure S26. ^1H NMR spectra of ISO, pure PIC and degradation mixture with $[\text{EminOH}]\text{Cl-2LA}$.

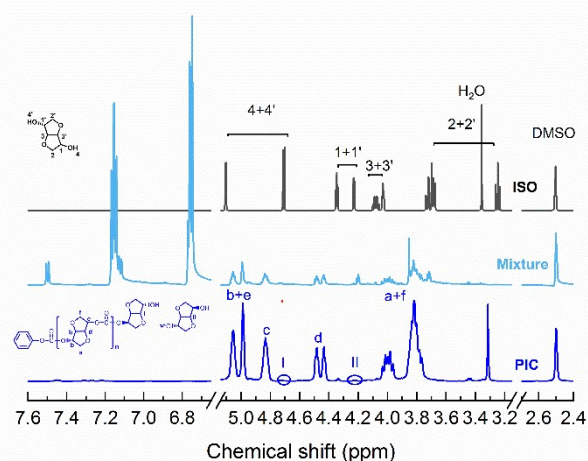


Figure S27. ^1H NMR spectra of ISO, pure PIC and degradation mixture with $[\text{EminOH}]\text{Cl-2PTSA}$.

Structural characterization of PIC

The detailed structure of the PIC prepared by $[\text{EminOH}]\text{Cl-2EG}$ was determined by ^1H NMR and ^{13}C NMR using CDCl_3 as the deuterated reagent. As was shown in Figure S30 (a), the chemical shifts of the hydrogen atoms labeled 3 and 4 in the repeating unit were 4.98 and 4.54 ppm, respectively. The characteristic peaks appearing at 5.06-5.16 represented the hydrogen atoms at 2 and 5. The peaks of 4 hydrogen atoms appearing at 3.91-4.07 ppm belonged to the chemical shifts of 1 and 6. The characteristic peak appearing at 2.55 ppm belonged to the derivatives of 1,4-sorbitan, a major substance that caused yellowing of PIC.^{1,2} Due to the existence of endo-hydroxyl groups and exo-hydroxyl groups in ISO, the carbon atoms on the carbonyl group of PIC had three shift peaks (Figure S18 (b)).³⁻⁵ The peaks at 154, 153.5 and 153 ppm were

derived from the carbon atoms of a₁, a₂ and a₃, respectively. Other characteristic peaks were respectively assigned to the carbon atoms on ISO in the repeating unit.

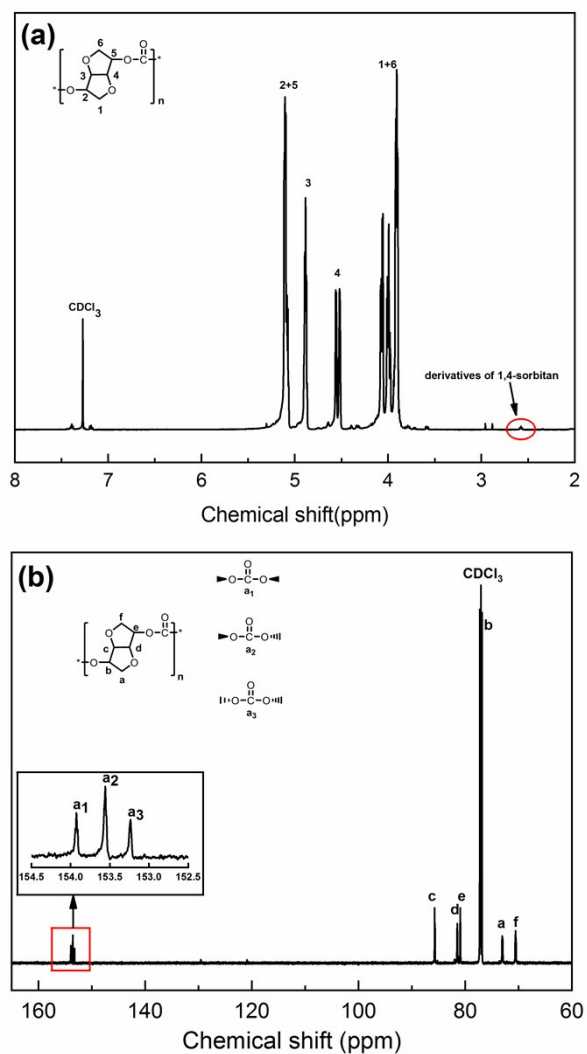


Figure S28. (a) ¹H NMR spectrum and (b) ¹³C NMR spectrum of PIC.

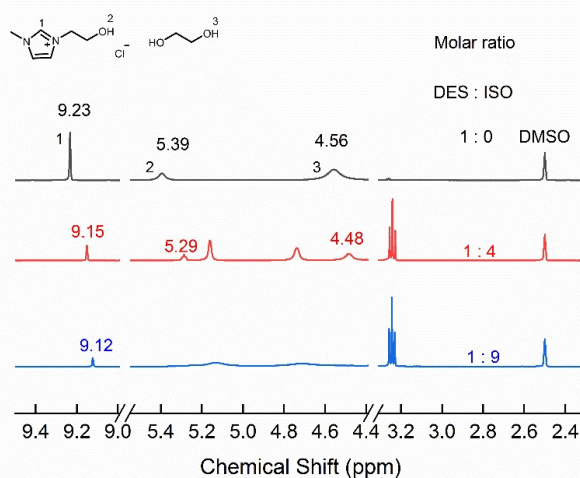


Figure S29. ¹H NMR spectra of ISO and [EminOH]Cl-2EG mixed in different molar ratios.

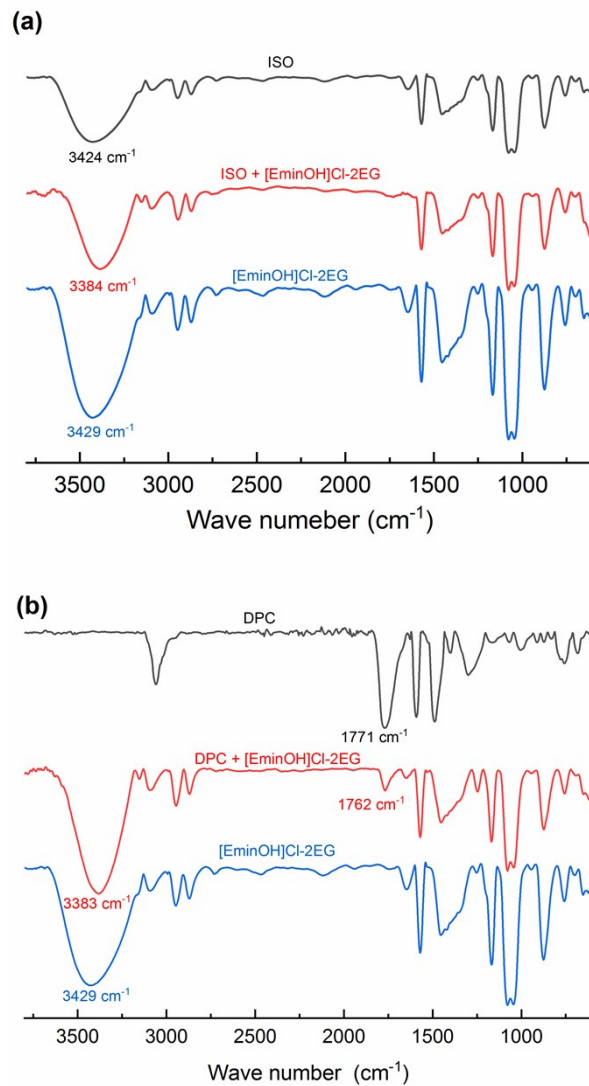


Figure S30. FT-IR spectra of (a) ISO with [EminOH]Cl-2EG and (b) DPC with [EminOH]Cl-2EG.

GPC data

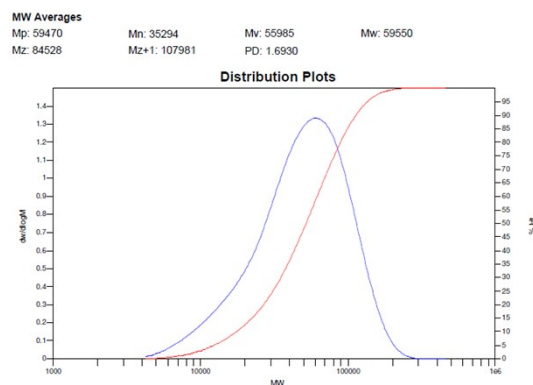


Figure S31. PIC synthesized by [EminOH]Cl.

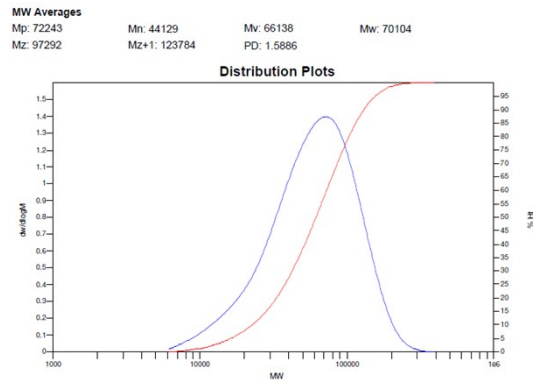


Figure S32. PIC synthesized by [EminOH]Cl-2TEOA.

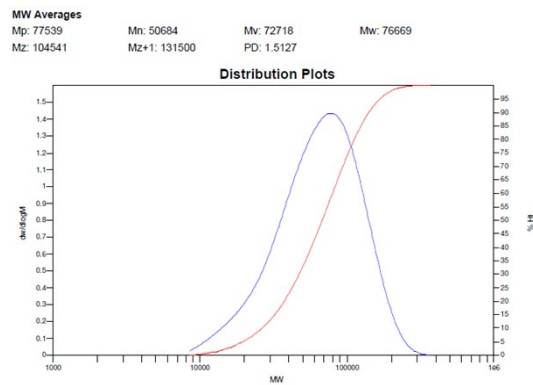


Figure S33. PIC synthesized by [EminOH]Cl-2IM.

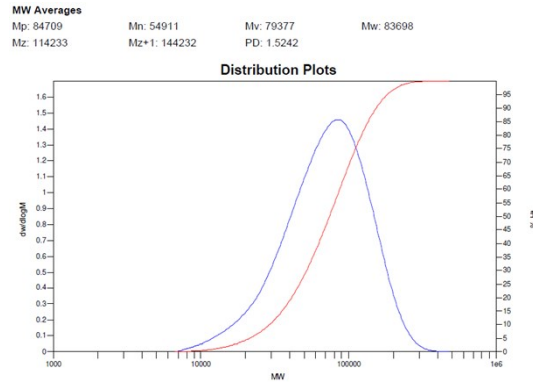


Figure S34. PIC synthesized by [EminOH]Cl-2UREA.

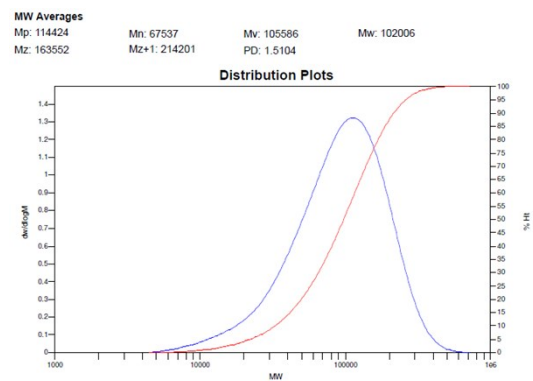


Figure S35. PIC synthesized by [EminOH]Cl-2EG.

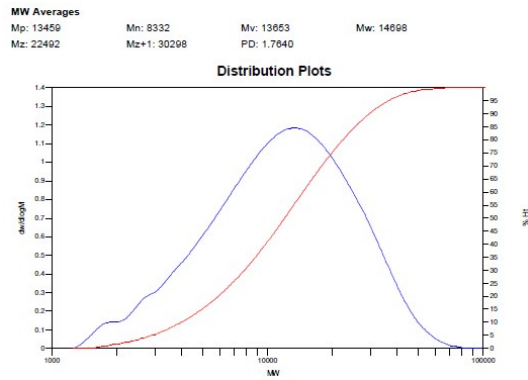


Figure S36. PIC synthesized by [EminOH]Cl-2LA.

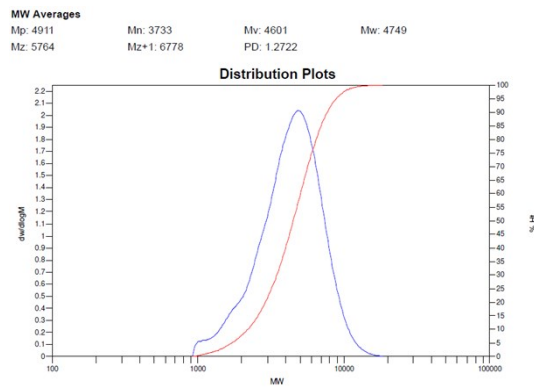


Figure S37. PIC synthesized by [EminOH]Cl-2PTSA.

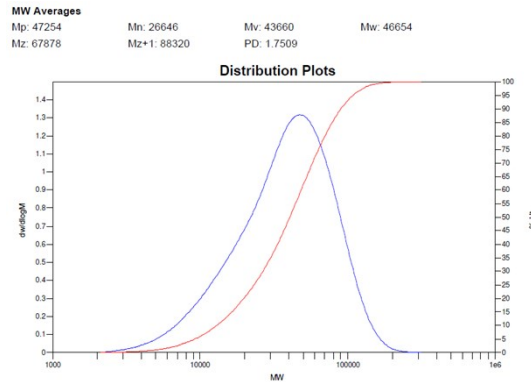


Figure S38. PIC synthesized by TEOA.

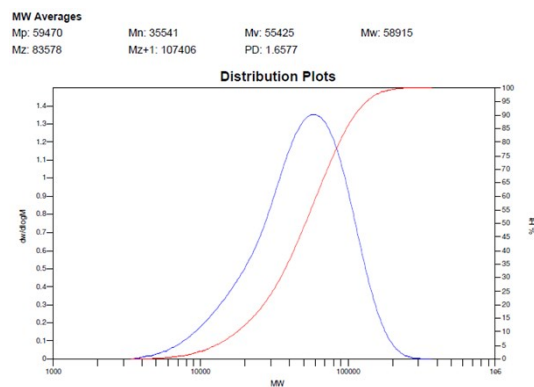


Figure S39. PIC synthesized by IM.

MW Averages
Mp: 47254 Mn: 27893 Mv: 44034 Mw: 46853
Mz: 66800 Mz+1: 86299 PD: 1.6797

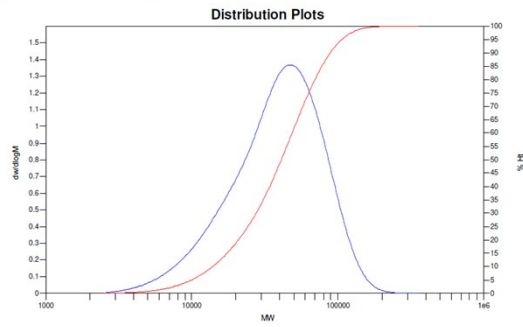


Figure S40. PIC synthesized by UREA.

MW Averages
Mp: 50718 Mn: 30093 Mv: 47287 Mw: 50278
Mz: 71344 Mz+1: 91660 PD: 1.6708

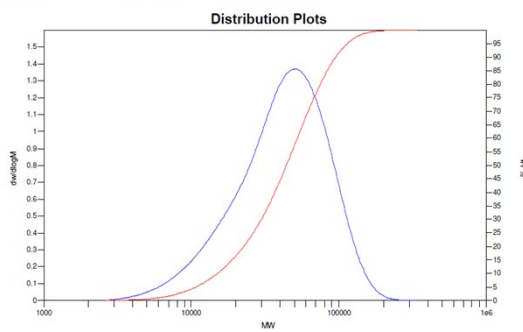


Figure S41. PIC synthesized by EG.

MW Averages
Mp: 22480 Mn: 13227 Mv: 22833 Mw: 21416
Mz: 37814 Mz+1: 52545 PD: 1.6191

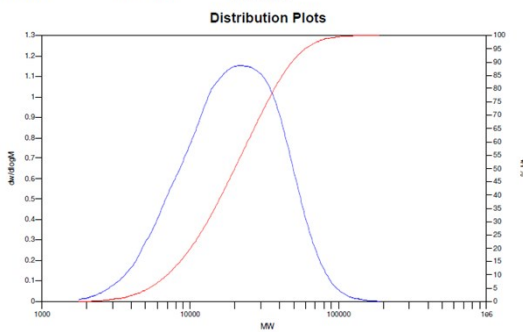


Figure S42. PIC synthesized by LA.

MW Averages
Mp: 4420 Mn: 3063 Mv: 4357 Mw: 4573
Mz: 10160 Mz+1: 17488 PD: 1.4929

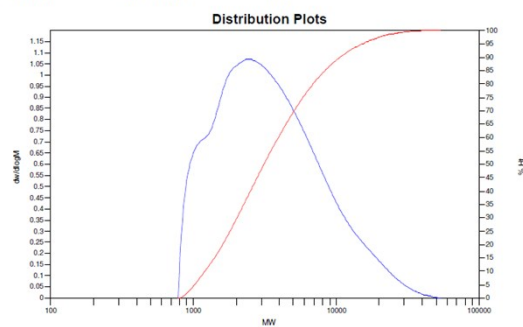


Figure S42. PIC synthesized by PTSA.

Reference

1. J. Hong, D. Radojicic, M. Ionescu, Z. S. Petrovic and E. Eastwood, *Polymer Chemistry*, 2014, **5**, 5360-5368.
2. J. M. Koo, S. H. Kim and S. S. Im, *Rsc Advances*, 2017, **7**, 6315-6322.
3. C. Ma, F. Xu, W. Cheng, X. Tan, Q. Su and S. Zhang, *ACS Sustainable Chemistry & Engineering*, 2018, **6**, 2684-2693.
4. Z. C. Zhang, F. Xu, Y. Q. Zhang, C. H. Li, H. Y. He, Z. F. Yang and Z. X. Li, *Green Chem.*, 2020, **22**, 2534-2542.
5. M. Zhang, W. Lai, L. Su and G. Wu, *Industrial & Engineering Chemistry Research*, 2018, **57**, 4824-4831.